

# Passive microwave-derived spatial and temporal variations of summer melt on the Greenland ice sheet

THOMAS L. MOTE, MARK R. ANDERSON, KARL C. KUIVINEN AND CLINTON M. ROWE  
*Department of Geography, University of Nebraska-Lincoln, Lincoln, NE 68588-0135, U.S.A.*

**ABSTRACT.** Passive microwave-brightness temperatures over the Greenland ice sheet are examined during the melt season in order to develop a technique for determining surface-melt occurrences. Time series of Special Sensor Microwave/Imager (SSM/I) data are examined for three locations on the ice sheet, two of which are known to experience melt. These two sites demonstrate a rapid increase in brightness temperatures in late spring to early summer, a prolonged period of elevated brightness temperatures during the summer, and a rapid decrease in brightness temperatures during late summer. This increase in brightness temperatures is associated with surface snow melting. An objective technique is developed to extract melt occurrences from the brightness-temperature time series. Of the two sites with summer melt, the site at the lower elevation had a longer period between the initial and final melt days and had more total days classified as melt during 1988 and 1989. The technique is then applied to the entire Greenland ice sheet for the first major surface-melt event of 1989. The melt-zone signal is mapped from late May to early June to demonstrate the advance and subsequent retreat of one "melt wave". The use of such a technique to determine melt duration and extent for multiple years may provide an indication of climate change.

## INTRODUCTION

Climate theory predicts, and climate models generally confirm, that temperature changes due to increased concentrations of radiatively active gases in the atmosphere will be greatest in high northern latitudes. Furthermore, a decrease in snow and ice cover in the Arctic may amplify any global warming by reducing the surface albedo and allowing Earth to absorb more solar radiation. Greater evaporation associated with increased temperatures in the Arctic may also lead to increased atmospheric moisture available for precipitation. In particular, the Greenland ice sheet may experience more accumulation due to increased atmospheric moisture and more ablation due to increased temperatures. An earlier and longer melt occurrence or greater spatial extent of surface melt should evidence an increase in the ice sheet's ablation. Therefore, surface melt could serve as a sensitive indicator of climate change. However, knowledge of the spatial and temporal extent of melt for the Greenland ice sheet is incomplete, in part due to the limited areal extent of surface observations spanning the onset and duration of summer melt.

Satellite remote sensing offers a means of measuring and monitoring the extent of surface melt on the Greenland ice sheet. In particular, microwave-brightness temperatures exhibit a distinct increase during surface melt. This peak in microwave emission stands in sharp contrast to the lower brightness temperatures observed under non-melt conditions for Greenland and Antarctica

(Gloersen and others, 1974). The rapid increase in brightness temperatures results from changing surface-snow conditions. It is well known that the emissivity of snow changes rapidly with melt, largely due to an increase in the water content of the snow (Chang and others, 1976; Rango and others, 1979; Foster and others, 1984; Chang and others, 1985). While snow density, temperature, crystal structure and crystal size all contribute to the snowpack's emissivity, changes in the volumetric water content produce the most prominent changes in brightness temperatures.

As the snowpack melts, liquid water forms between the individual snow grains, which increases the absorption and decreases the volume scattering (Rango and others, 1979). The surface scattering is enhanced over the volume scattering by two orders of magnitude (Mätzler and others, 1984). The result is a substantial increase in the emissivity of the snow. Snow with 1–2% liquid-water content may produce 37 GHz brightness temperatures 50 K higher than dry snow (Hofer and Mätzler, 1980). Experimental work has been conducted to describe the relationship between liquid-water content and microwave-brightness temperatures. Stiles and Ulaby (1980) empirically fit an exponential function of the form:

$$T_B(m_v) = A - Be^{-cm_v} \quad (1)$$

where  $T_B$  = microwave-brightness temperature and  $m_v$  = liquid water content, for liquid-water content between 0 and 6%. The greatest increase in brightness temperatures occurs from snow with 0.5–1% liquid-water

content (Stiles and Ulaby, 1980). This conspicuous signal and its usefulness as an indicator of climate variability, and thus climate change, has led to repeated calls for scientists to map the melt zones of the ice sheets (Zwally, 1977; Thomas, 1991).

The availability of more than a decade of passive microwave data now provides a viable method of mapping the melt zone and observing the intra- and inter-annual variability of surface melt. This paper examines time series of passive microwave data during the melt season for locations within the wet- and dry-snow zones of the ice sheet. From the time series, an objective technique for determining surface melt is developed. This technique is used to map the melt-zone signal as it advances across the ice sheet during the late spring of 1989.

**MICROWAVE DATA**

Passive microwave data used to determine the melt zone were acquired from the Special Sensor Microwave/

Imager (SSM/I), a second-generation multichannel microwave radiometer. The SSM/I records radiation in seven channels, the vertical and horizontal polarizations for 19.35 GHz (1.55 cm), 37.0 GHz (0.81 cm) and 85.5 GHz (0.35 cm) and the vertical polarization for 22.235 GHz (1.35 cm). The first SSM/I, launched on 19 June 1987, has a sun-synchronous, near-polar orbit with an altitude of 883 km, a swath width of 1400 km and a view angle of 53.1° (Hollinger and others, 1987).

The SSM/I data used in this study, from July 1987 to June 1990, were obtained from the National Snow and Ice Data Center's (NSIDC) archive of brightness temperature grids on compact disc. The 19 and 37 GHz data used in this investigation have been binned by NSIDC into a 25 km × 25 km grid. The binning process averages all observations that fall within the grid cell for each day, midnight to midnight UTC (National Snow and Ice Data Center, 1992). The coastal mask supplied with the SSM/I data was applied to eliminate pixels containing both land and water. However, pixels along the ice-sheet edge that contain land or both land and ice have not been removed from the data.

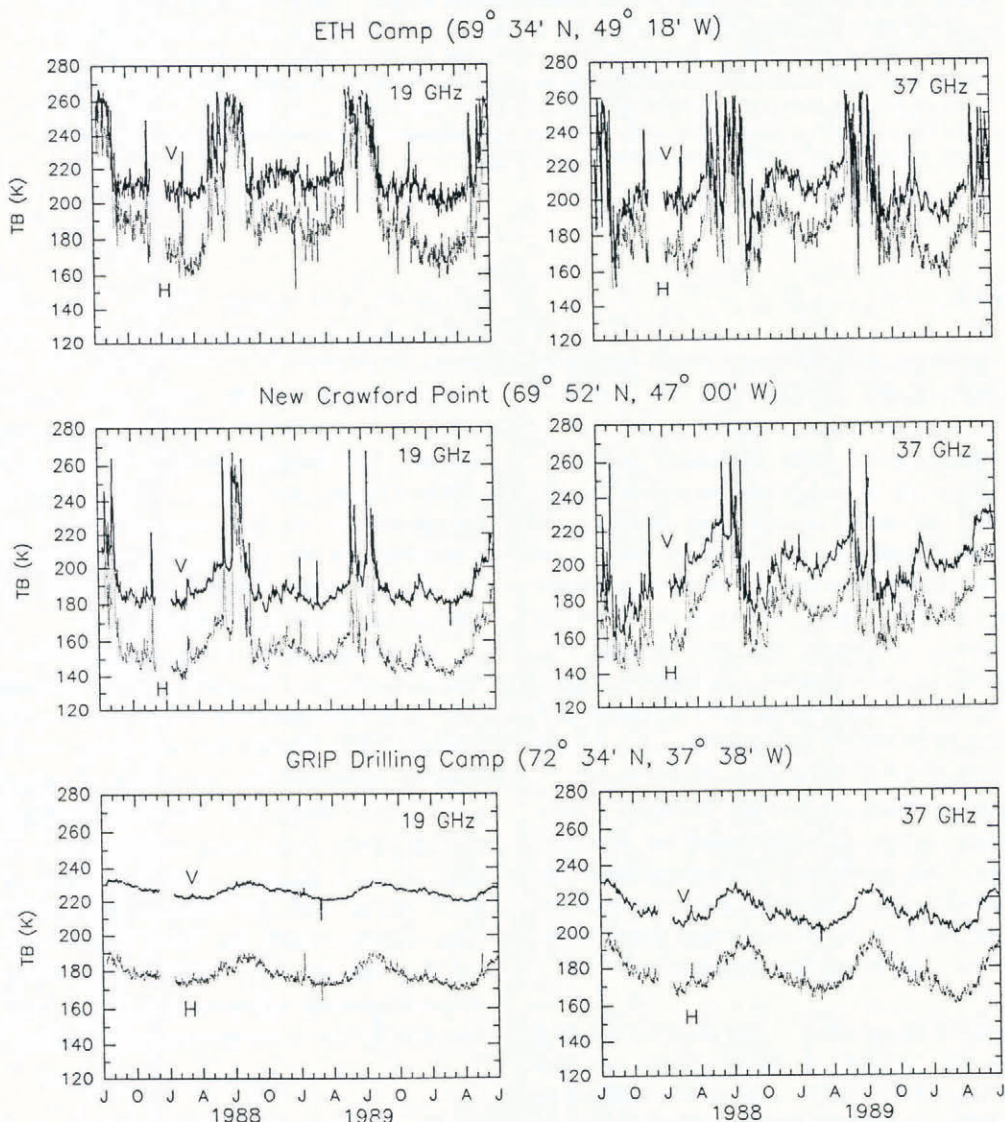


Fig. 1. Microwave-brightness temperature time series of the vertically and horizontally polarized channels at 19 and 37 GHz for three locations on the Greenland ice sheet.

## EXAMINATION OF MICROWAVE MELT SIGNAL

To develop an understanding of surface melt as identified by passive microwave data, time series of SSM/I microwave-brightness temperatures were produced for three locations on the ice sheet. The locations were selected from previously occupied research sites: the Swiss Federal Institute of Technology (ETH) camp (69°34' N, 49°18' W; 1175 m a.s.l.), NASA's camp at New Crawford Point (69°52' N, 47°00' W; 1879 m a.s.l.) and the European GRIP deep ice-core drilling camp (71°34' N, 37°38' W; 3230 m a.s.l.). The ETH camp is of particular interest because published data on snowpack characteristics at that location by Ohmura and others (1991) overlap the available microwave data by one month, allowing some limited comparison.

The GRIP drilling camp, near the summit of the ice sheet, lies in the dry-snow zone and is generally believed never to experience surface melt. However, the ETH camp lies near the equilibrium line and New Crawford Point lies in the percolation zone; accordingly, both sites are subject to summer surface melt. New Crawford Point experiences a rapid change from the dry-snow condition of winter to the percolation of melt water during the summer, but no melt ponds formed during surface observations in June and August 1991 (personal communication from K. Jezek). At the ETH site, supraglacial lakes were observed during the summer of 1990. Surface drainage channels formed, and surface lakes filled with water by late June (Laternser, 1991).

Under the assumption that these sites are representative of wet- and dry-snow zones, time series of brightness temperatures for four channels (19V/H, 37V/H) were constructed from three years of SSM/I data (Fig. 1). These time series were examined for differences between microwave signals from locations with and without summer melt.

The most prominent features in the time series for the ETH and New Crawford Point sites are the rapid increases in brightness temperatures during late spring to early summer, the prolonged period of elevated brightness temperatures during the summer, and the rapid decrease in brightness temperatures during late summer (Fig. 1). For example, the 19V brightness temperatures for the ETH site demonstrate a rapid decline in August 1987 from values around 260 K in the summer to approximately 210 K during the winter. A rapid increase in the brightness temperatures occurs at the end of May 1988 and continues through the summer with a subsequent decline in August. This pattern is repeated for the remainder of the time series and a comparable pattern is observed in the 19H channel.

Similar transitions between seasons are observed in the vertical and horizontal 37 GHz brightness temperatures, although greater variability is present within each season for these channels. Most of the gradual increase in brightness temperatures throughout the spring is probably the result of increasing snowpack temperatures. However, examination and discussion of the smaller-scale variability is beyond the scope of this paper.

Large variations are also observed in the brightness temperatures for the New Crawford Point site (Fig. 1), though the summer plateaus are not as prolonged as those

observed at the ETH site. The highest summer brightness temperatures are similar at the ETH and New Crawford Point sites. Other locations on the ice sheet had brightness temperatures near 273 K, which result from the emissivity of near unity for wet snow with a volumetric water content greater than 2%. Maximum brightness temperatures of approximately 260 K for the ETH and New Crawford sites during surface melt result from an emissivity of less than one and may be a result of liquid-water content between 0.5 and 2%, in addition to any remaining dry snow within the foot print of the sensor.

Although no rapid changes or periods of elevated brightness temperatures occur during the three-year period for the GRIP drilling site as was observed for the ETH or New Crawford Point sites (Fig. 1), the annual temperature cycle is clearly present in the brightness-temperature time series. The seasonal variation in temperature is more pronounced in the 37 GHz channels than the 19 GHz channels. For example, exclusive of the melt period, the 19V brightness temperatures range from 220 to 235 K, whereas the 37V brightness temperatures range from 200 to 230 K. This is likely due to the fact that radiation received at 19 GHz emanates from a deeper and more thermally stable layer of the snowpack than radiation at 37 GHz.

## OBJECTIVE MELT DETERMINATION

In order to catalogue melt onset, duration and accumulated melt days objectively, one channel was selected to identify the brightness temperature peak. The goal in selecting that channel was to minimize the within-melt variance of the brightness temperatures and maximize the melt-non-melt difference. The brightness temperature time series for the ETH site was used to determine means and standard deviations (Table 1) separately for a winter period (1 December 1988–28

Table 1. Means and standard deviations of brightness temperatures for the ETH site

1 December 1988 – 28 February 1989				
	19V	19H	37V	37H
Mean	214.2	186.5	210.1	184.3
S.D.	5.9	7.8	5.6	6.8
1 June 1989 – 31 July 1989				
	19V	19H	37V	37H
Mean	255.1	237.8	234.5	221.1
S.D.	10.0	12.7	23.8	24.9

February 1989) and a melt period (1 June 1989–31 July 1989). The 19V channel demonstrates the greatest difference of the means between winter and the summer melt (41 K) and has the smallest standard deviation during the melt (10 K). Therefore, the 19V channel was selected to serve as an indicator of melt.

The difference between the 19V summer and winter means was used as the basis to determine the melt threshold for two reasons. First, the differencing technique accounts for observed variations in brightness temperatures across the ice sheet prior to the onset on summer melt. Secondly, employing this difference aids in eliminating coastal land contamination due to the smaller variation in brightness temperatures for land surfaces than for snow and ice surfaces. A threshold of 31 K above the winter mean was derived by subtracting one standard deviation of the melt-period brightness temperatures from the difference in means. This was done to avoid indicating a return to non-melt conditions due to the smaller-scale variations observed during the melt period.

**MELT FEATURES**

The brightness temperature threshold of 31 K above the winter mean is used to identify melt periods for the ETH camp and New Crawford Point for the three years of available SSM/I data. Any day with a brightness temperature greater than the threshold was classified as melt. The length of melt, or melt season, can then be determined by the number of days between the first observation above the threshold and the last day above the threshold.

*Table 2. Melt dates between 10 July 1987 and 30 June 1990 from SSM/I data for the ETH and New Crawford Point sites*

	<i>ETH Camp</i>		<i>New Crawford Point</i>	
	<i>Begin</i>	<i>End</i>	<i>Begin</i>	<i>End</i>
1987		15 Aug		23 Jul
1988	15 May	17 May	9 Jun	13 Jun
	28 May	30 May	4 Jul	5 Aug
	9 Jun	16 Jun		
	29 Jun	3 Aug		
	6 Aug	21 Aug		
1989	30 May	30 Jun	30 May	2 Jun
	4 Jul	13 Aug	9 Jun	13 Jun
	17 Aug	19 Aug	14 Jul	27 Jul
1990	7 May	9 May	20 Jun	26 Jun
	29 May	1 Jun		
	8 Jun	12 Jun		
	16 Jun			

In 1988 and 1990, the first day above the threshold, the melt onset, occurred earlier at the grid cell containing the ETH site than at the New Crawford Point grid cell (Table 2). However, during 1989 the melt onset occurred on 30 May at both grid cells. The ending date for the melt season occurred on different dates for the two sites each year. In general, the last day of melt for the New Crawford Point grid cell is 20 d earlier than for the ETH site (Table 2). The earlier onset and later ending date resulted in a longer melt season for the ETH site than for the New Crawford Point site. The 1988 melt season lasted 99 d at the ETH site and 58 d at the New Crawford Point site. The 1989 melt season lasted 82 d at the ETH site and 59 d at the New Crawford Point site. The difference in the length of the melt season between the two grid cells is likely related to the elevation difference between the two locations.

During the melt season, the brightness temperatures fall below the threshold value on a number of days. This implies that the total length of the melt season may not fully characterize the duration of surface melt for each grid cell. Therefore, the total number of days classified as melt during each season, referred to here as the number of accumulated melt days, is also determined for the two sites. During both 1988 and 1989, the ETH site had more accumulated melt days than New Crawford Point. The ETH site had 76 melt days as opposed to 38 for the New Crawford Point in 1988 and 66 melt days as opposed to 23 for New Crawford Point in 1989. For the two years examined, a large inter-annual variability exists for both sites.

During June 1990, simultaneous daily ground observations were available for the ETH site (Greuell and Konzelmann, 1991). This overlap permits a comparison between the microwave-brightness temperatures and several surface parameters, particularly the water content of the snow. Due to the coarse resolution of the microwave grid, some caution must be exercised in relating the microwave data to surface observations. Nevertheless, there is close agreement between onset of the first continuous microwave peak and the published data on mean liquid-water content of the snowpack. The first continuous peak in emission for 1990 begins on 16 June, the same day the liquid-water content at the ETH camp was first reported greater than 2%. The microwave-brightness temperatures continued to rise until 24 June. Concurrently, the reported volumetric water content increased until it reached a June peak of 5.51% on 23 June (Greuell and Konzelmann, 1991). This comparison supports the conclusion that the volumetric water content of the snowpack is the dominant factor in the microwave signature during melt and therefore can be used to identify melt. Two 4 d peaks and one 5 d peak are evident in the time series between mid-May and early June, before the period of continuous summer melt. These shorter-lived peaks are likely due to radiation melting of the surface. Greuell and Konzelmann (1991) reported evidence of surface melting at the ETH camp as early as 24 May but no measurements of snow properties are available for May.

To assess the usefulness of the objectively determined threshold, the 31 K difference threshold was applied to each grid cell over Greenland to map the advance and

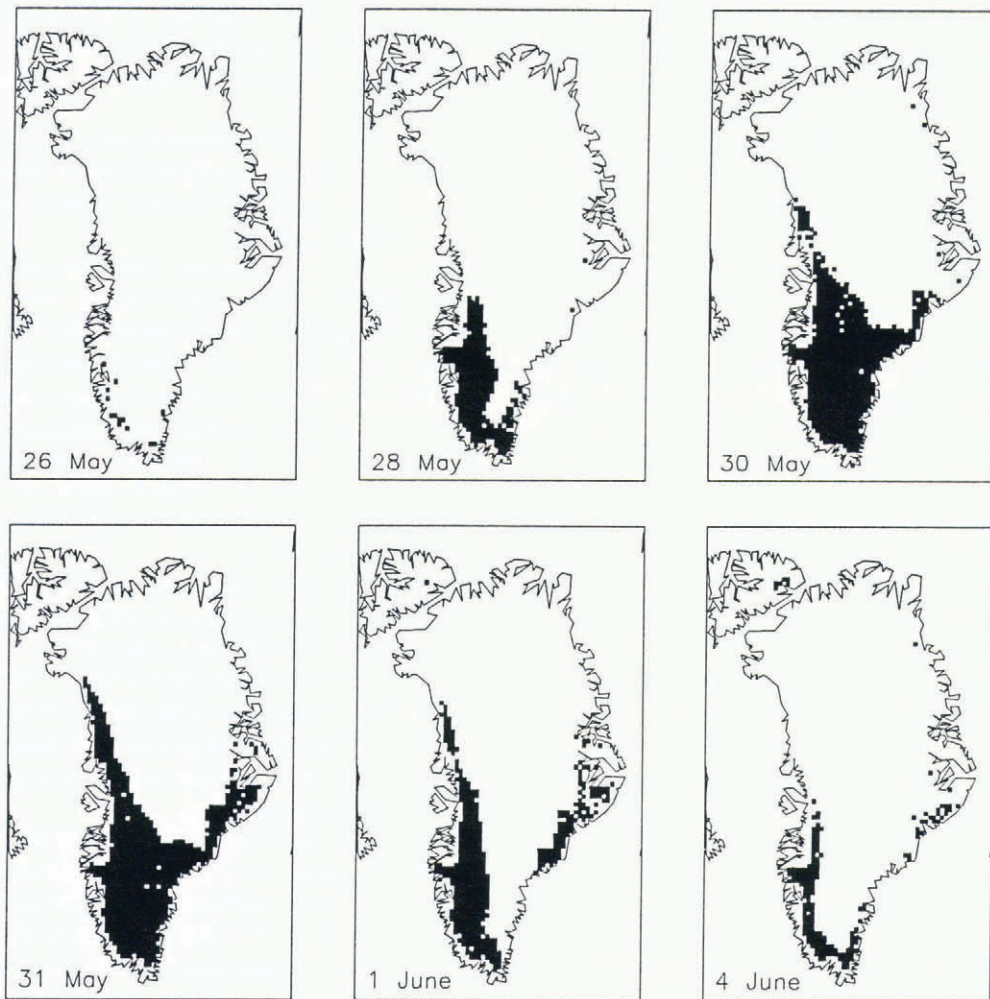


Fig. 2. Microwave-derived surface melt extent (in black) during the first major surface melt event of 1989.

retreat of one “melt wave” during late May and early June 1989. To display the spatial extent of melt, difference maps were produced using individual summer images and the 20 January 1989 image, which served as a proxy for the mean winter conditions across the entire ice sheet. Zhang and others (1989) have shown that microwave-brightness temperatures are stable throughout winter across the Greenland ice sheet; thus, a single winter image can provide a first approximation to the mean winter conditions. If the summer–winter difference for an individual grid cell exceeded 31 K, the cell was classified as experiencing melt.

A sequence of six melt-extent maps, concentrating on the period of rapid increase in melt during late May 1989, was produced (Fig. 2). The 26 May map shows only isolated grid cells in the southwestern part of the ice sheet classified as experiencing surface melt. The number of grid cells classified as melt dramatically increased between 28 and 30 May. By 30 May, the entire southern dome and much of the western edge of the ice sheet were classified as experiencing surface melt. The number of grid cells classified as melting began to decline through the last image on 4 June, when only the periphery of the ice sheet remained classified as melting. As expected, the melt advance approximately followed the elevation contours of the ice in southern Greenland due to the

dependence of temperature on elevation. This agrees with the dependence of melt on elevation evident in the comparison of brightness-temperature time series for the ETH and New Crawford Point sites.

## SUMMARY AND CONCLUSIONS

Time series of SSM/I data for two sites in the wet-snow zone demonstrate a rapid increase in brightness temperatures during late spring to early summer, a prolonged period of high brightness temperatures during the summer and a rapid decrease in late summer. Previous research on the microwave emission of snow as well as knowledge of the surface conditions at the two sites suggests that the peaks are associated with melting of surface snow.

A threshold based on a comparison of summer and winter time series was developed to classify melt events. This technique was applied to the two wet-snow sites, and it classified a longer and more continuous melt season at the ETH camp, the lower elevation site, than the New Crawford Point site. Additionally, corresponding surface and microwave observations during June 1990 seem to demonstrate a relationship between the volumetric water content of the snowpack and the increase in brightness

temperature. Earlier, short-lived peaks that are evident in the time series cannot be attributed directly to increases in the liquid-water content due to a lack of concurrent surface observations. These peaks may be due to localized radiation melting of the top snow layer.

An objective technique to determine melt was applied to the entire ice sheet for a 10 d period in late May and early June 1989. The results demonstrate a rapid melt advance across the ice sheet, approximately following elevation contours.

Further refinement of the technique for determining melt events from passive microwave data is warranted. This refinement process should involve co-ordinated surface and satellite observations. Additionally, the small-scale variability evident in the time series needs further examination. Following additional refinements, Scanning Multichannel Microwave Radiometer (SMMR) and Electronically Scanning Microwave Radiometer (ESMR) data could be employed to provide a sufficiently long time series to map the inter-annual variability of melt extent on the ice sheet. This should prove a valuable addition to the effort to understand climate variability and, possibly, to detect climate change.

#### ACKNOWLEDGEMENTS

This work was partially supported by NASA grant NAGW-1266. The SSM/I gridded brightness-temperature data on CD-ROM were obtained from the National Snow and Ice Data Center, Boulder, Colorado, U.S.A.

#### REFERENCES

- Chang, T. C., P. Gloersen, T. Schmugge, T. T. Wilheit and H. J. Zwally. 1976. Microwave emission from snow and glacier ice. *J. Glaciol.*, **74**(16), 23–39.
- Chang, A. T. C., J. L. Foster, M. Owe, D. K. Hall and A. Rango. 1985. Passive and active microwave studies of wet snowpack properties. *Nord. Hydrol.*, **16**(2), 57–66.
- Foster, J. L., D. K. Hall, A. T. C. Chang and A. Rango. 1984. An overview of passive microwave snow research results. *Rev. Geophys. Space Phys.*, **22**(2), 195–208.

- Gloersen, P., T. T. Wilheit, T. C. Chang, W. Nordberg and W. J. Campbell. 1974. Microwave maps of the polar ice of the Earth. *Bull. Am. Meteorol. Soc.*, **55**(12), 1442–1448.
- Greuell, W. and T. Konzelmann. 1991. Mass budget. In *ETH Greenland Expedition. Progress Report No. 1: April 1990 to February 1991*. Zürich, Swiss Federal Institute of Technology, 83–93.
- Hofer, R. and C. Mätzler. 1980. Investigations on snow parameters by radiometry in the 3- to 60-mm wavelength region. *J. Geophys. Res.*, **85**(C1), 453–460.
- Hollinger, J., R. Lo, G. Poe, R. Savage and J. Peirce. 1987. *Special sensor microwave/imager user's guide*. Washington, DC, Naval Research Laboratory.
- Latnser, M. 1991. Surface morphology. In *ETH Greenland Expedition. Progress Report No. 1: April 1990 to February 1991*. Zürich, Swiss Federal Institute of Technology, 17–20.
- Mätzler, C., H. Aebischer and E. Schande. 1984. Microwave dielectric properties of surface snow. *IEEE J. Oceanic Eng.*, **OE-9**(5), 366–371.
- National Snow and Ice Data Center. 1992. *DMSP SSM/I brightness temperature grids for the polar regions on CD-ROM. User's guide*. Boulder, CO, University of Colorado. Cooperative Institute for Research in Environmental Sciences.
- Ohmura, A. and 8 others. 1991. *ETH Greenland Expedition. Progress Report No. 1: April 1990 to February 1991*. Zürich, Swiss Federal Institute of Technology.
- Rango, A., A. T. C. Chang and J. L. Foster. 1979. The utilization of spaceborne microwave radiometers for monitoring snowpack properties. *Nord. Hydrol.*, **10**(1), 25–40.
- Stiles, W. H. and F. T. Ulaby. 1980. The active and passive microwave response to snow parameters. 1. Wetness. *J. Geophys. Res.*, **85**(C2), 1037–1044.
- Thomas, R. H. 1991. *Polar research from satellites*. Washington, DC, Joint Oceanographic Institutions, Inc.
- Zhang, H., L. Tondal Pedersen and P. Gudmandsen. 1989. Microwave brightness temperatures of the Greenland ice sheet. *Adv. Space Res.*, **9**(1), 277–287.
- Zwally, H. J. 1977. Microwave emissivity and accumulation rate of polar firn. *J. Glaciol.*, **18**(79), 195–215.

*The accuracy of references in the text and in this list is the responsibility of the authors, to whom queries should be addressed.*